HHS Public Access

Author manuscript

J Cardiovasc Electrophysiol. Author manuscript; available in PMC 2021 February 26.

Published in final edited form as:

J Cardiovasc Electrophysiol. 2017 October ; 28(10): 1158–1166. doi:10.1111/jce.13283.

Rotors Exhibit Greater Surface ECG Variation during Ventricular Fibrillation than Focal Sources due to Wavebreak, Secondary Rotors, and Meander

Gordon Ho, MD[1,2], **Christopher T. Villongco, PhD**[3], **Omid Yousefian, MD**[4], **Aaron Bradshaw, BS**[5], **Andrew Nguyen, MD**[1,2], **Yonatan Faiwiszewski, MD**[1,2], **Justin Hayase, MD**[1,2], **Wouter-Jan Rappel, PhD**[6], **Andrew D. McCulloch, PhD**[1,3], **David E. Krummen, MD, FHRS**[1,2]

[1]Dept. of Medicine, University of California San Diego

[2]Veterans Affairs San Diego Healthcare System, San Diego, CA

[3]Dept. of Bioengineering, University of California San Diego

[4]Dept. of Medicine, University of Southern California, Los Angeles, CA

[5]UCSD School of Medicine, San Diego, CA

[6]Dept. of Physics, University of California San Diego

Abstract

Introduction—Ventricular fibrillation is a common life-threatening arrhythmia. The ECG of VF appears chaotic but may allow identification of sustaining mechanisms to guide therapy.

Hypothesis—We hypothesized that rotors and focal sources manifest distinct features on the ECG, and computational modeling may identify mechanisms of such features.

Methods—VF induction was attempted in 31 patients referred for ventricular arrhythmia ablation. Simultaneous surface ECG and intracardiac electrograms were recorded using biventricular basket catheters. Endocardial phase maps were used to mechanistically classify each VF cycle as rotor or focally-driven. ECGs were analyzed from patients demonstrating both mechanisms in the primary analysis and from all patients with induced VF in the secondary analysis. The ECG voltage variation during each mechanism was compared. Biventricular computer simulations of VF driven by focal sources or rotors were created and resulting ECGs of each VF mechanism were compared.

Results—Rotor-based VF exhibited greater voltage variation than focal source-based VF in both the primary analysis (n=8, 110±24% vs 55±32%, p=0.02) and the secondary analysis (n=18, 103±30% vs 67±34%, p=0.009). Computational VF simulations also revealed greater voltage

Correspondence to: Gordon Ho, MD, 3350 La Jolla Village Drive, Cardiology Section 111A, San Diego CA, 92161, Office: 858-642-3889, Fax: 858-552-7490, goho@ucsd.edu.

Dr. Krummen has served as a consultant to Abbott Inc., and has received fellowship program support from Biosense-Webster, Biotronik, Boston Scientific, Medtronic, and St. Jude. Dr. Rappel is a coinventor on intellectual property owned by the University of California and licensed to Abbott. Dr. McCulloch has intellectual property and ownership interest in InSilicoMed Inc. Other authors: No disclosures.

variation in rotors compared to focal sources (110±19% vs 33±16%, p=0.001), and demonstrated that this variation was due to wavebreak, secondary rotor initiation, and rotor meander.

Conclusion—Clinical and computational studies reveal that quantitative criteria of ECG voltage variation differ significantly between VF-sustaining rotors and focal sources, and provide insight into the mechanisms of such variation. Future studies should prospectively evaluate if these criteria can separate clinical VF mechanisms and guide therapy.

Keywords

Ventricular fibrillation; Rotors; Electrocardiography; Catheter ablation; Phase mapping; Patient specific computational modeling

Introduction

Ventricular fibrillation (VF) remains an important public health problem, accounting for significant morbidity and mortality.[1, 2] While multiple mechanisms underlying human VF have been proposed,[3-7] spiral waves (rotors) and focal sources are of particular interest because they may be amenable to targeted therapies such as ablation.[8, 9] However, identification of such sources during VF has required invasive 64-electrode endocardial basket catheters[9, 10] or a multielectrode mapping vest.[11]

Currently, ECG tracings of non-VF arrhythmias are routinely evaluated by clinicians to determine the presence and location of underlying mechanisms. However, the ECG of VF is challenging to interpret. In prior work, quantitative analysis of the ECG during long duration VF demonstrated the progression of VF amplitude and frequency over time.[12] Additionally, low amplitude VF (fine VF) was associated with sustained episodes. However, at present there is no method to extract information regarding VF source type or temporal stability.

We hypothesized that rotors and focal sources would manifest distinct features on the surface 12-lead ECG during VF. We further hypothesized that realistic computer simulation can evaluate the underlying mechanisms responsible for observed differences. Such information may help guide future classification and directed therapy of arrhythmia-sustaining mechanisms in patients with clinical VF.

Methods

Patient Enrollment

For the clinical study, we enrolled consecutive patients presenting for ventricular arrhythmia ablation at the University of California San Diego and VA San Diego Healthcare System. The protocol was approved by the institutional review boards (IRBs) at each institution, and all patients provided written, informed consent. Exclusion criteria were the presence of ventricular thrombus, hemodynamic instability precluding the safe induction of VF, and significant, unrevascularized coronary ischemia.

Antiarrhythmic drugs were discontinued greater than 5 half-lives (6 weeks for amiodarone) prior to electrophysiology study. LV function was assessed by transthoracic echocardiography prior to the procedure.

Clinical Study Protocol

The clinical study protocol has been previously described.[9, 10] In summary, patients were sedated and ventilated under a consistent general anesthesia protocol. Next, a decapolar catheter was placed in the coronary sinus, an intracardiac echocardiographic (ICE) catheter placed in the right atrium, and a quadripolar catheter was placed in the right ventricle (RV) for VF induction. Basket catheters (64-electrode, Constellation, Boston Scientific, Natick, MA) were advanced for simultaneous recording into the RV and left ventricle (LV). Following baseline programmed ventricular stimulation, rapid pacing was performed for 15 seconds, followed by a 1-minute recovery period, for each cycle length (CL) of 350, 300, 250, then decrementing by 10 msec until VF induction or 2:1 capture (minimum CL 170 msec), per protocol.[13] As soon as VF was induced, defibrillator charging commenced, and VF was recorded during this charging period. VF was defibrillated as soon as charging was complete (11.4±2.9 seconds; range 8-15 seconds). After a 5-minute waiting interval, a second episode of VF was induced in each patient either with a second burst pacing induction, or with 3.2 seconds of rapid pacing followed by a 2 Joule T-wave shock in patients with ICDs. VF was defined as varying ECG morphology with a rate >220 beats per minute as previously defined.[14] Following the second attempted VF induction, the clinical procedure was commenced in routine fashion.

Mechanistic Classification of VF Using Endocardial Phase Maps

Unipolar electrograms (Bard Pro, Billerica, MA) were recorded at 1000 Hz and filtered from 0.05 to 500 Hz. Multipolar basket electrograms were analyzed offline using software that we have developed and described previously[15] and optimized for VF analysis, using phase analysis[16] of unipolar electrograms,[7] within physiologic constraints.[17, 18] Data were analyzed for the first 10 seconds of VF or until termination, whichever came first.

Rotors were defined as regions of rotational activity that controlled surrounding activation and associated with a phase singularity formed at the intersection of depolarization and repolarization isolines[6] consisting of at least 1 rotation. Phase singularities were identified quantitatively using phase mapping by identifying areas of activation in which the phase of all surrounding points were equal. The software represented these phase singularities by a white or red dot. We defined stable phase singularities as those visible for the entirety of 1 or more VF cycles. Focal sources were defined as regions of centrifugal activation propagating away from a single point without rotation (e.g., without phase singularities during phase analysis). Example phase maps of each are demonstrated in Video 1.

Metrics for Surface ECG Voltage Variation Analysis

All ECGs were normalized in order to eliminate confounding structural and functional differences between patients that can affect absolute ECG amplitude (such as the torso and presence of left ventricular hypertrophy). This step eliminates the need to simulate fixed factors that affect the absolute voltage amplitude, such as the torso, and enables the use of a

monodomain electrophysiology computer model. Next, the peak-to-trough amplitude of every VF cycle was measured from orthogonal leads I, aVF and V1 in each pre-classified VF episode. ECG voltage variation was then evaluated using 2 quantitative metrics: the first metric measures the percent difference between the largest and smallest amplitude measured from all VF cycles. The second metric measures the standard deviation of the amplitudes measured from all VF cycles, normalized to the mean amplitude. To evaluate 3-dimensional voltage differences, the vector-sum of the amplitudes from the orthogonal leads (calculated as the square root of the sum of squares of the amplitudes from the orthogonal leads) were compared.

Human Clinical Study of VF Mechanisms on ECG

In the clinical study, standard 12-lead surface ECGs and endocardial phase maps were recorded simultaneously during each episode of induced VF. The raw digitized surface electrograms were taken from the Bard system (Bard Pro, Billerica, MA) and imported into Matlab (Mathworks, Boston, MA) for analysis. Sustained VF was defined as episodes with duration at least 10 seconds and requiring defibrillation. After classifying each VF cycle according to VF mechanism determined from endocardial phase maps, periods of only rotors vs only focal sources were identified. Using the above voltage variation metrics, ECGs from these VF periods were analyzed. In the primary analysis, ECGs were analyzed only from patients who exhibited both VF mechanisms in order to control for structural and functional differences between patients. In the secondary clinical analysis, episodes from all patients with induced VF were analyzed.

Computational Modeling Study

Detailed biventricular computational simulations were constructed using a high order cubic-Hermite finite element mesh consisting of 76,000 elements (spatial resolution $\Delta x=2mm$) derived from the study patients' thoracic computed tomography scans (CT), as demonstrated in Figure 1.[19, 20] Ventricular fiber architecture was approximated by mapping fiber orientations measured by diffusion tensor magnetic resonance imaging (DT-MRI) in an excised human heart to the patient ventricular geometry.[21]

Using the Fenton-Karma electrophysiology model[22] and monodomain wave propagation, spiral waves and ectopic focal sources were simulated. A total of nine rotor simulations were performed, each with a single spiral wave originating from a different ventricular location. Six of the rotor simulations were performed at a physiologic conduction velocity of 0.002 cmˆ2/ms, with three simulations eventually forming multiple secondary rotors and three simulations forming meandering rotors. Three of the rotor simulations were performed at a non-physiologic conduction velocity of 0.01 cmˆ2/ms that resulted in a single rotor fixed at a stationary ventricular location. Next, a total of three series of focal source simulations were performed, each with an ectopic stimulus site located in a different ventricular location. The point stimulus was set to fixed pacing cycle length of 200ms, similar to the VF cycle length observed in the clinical study, with small variation in source location as observed clinically. All other parameters were controlled such as mesh geometry and electrophysiological properties. The base physiologic parameter set used for the Fenton–Karma model was parameter set 3 in Fenton et al.[22] to mimic VF-like behavior with steep APD restitution

curve. The excitability value of the model was represented by $g_{fi,}$ which is the reciprocal of tau_d which is the time constant that controls the speed of the upstroke of the action potential ($g_{fi} = 1/tau_{d,}$). In our models, g_{fi} was set at 2.95 ms^{-1} to create spiral waves that rotated at a frequency of 4-5 Hz, approximately equal to that observed in patients in our clinical study. To account for decreased anisotropy of conduction in diseased, remodeled myocardium, a transversely isotropic conductivity tensor was used with components of D_{fibre} = 0.4 mm^2/ms and $D_{cross\text{-}fibre}$ = 0.1 mm^2/ms.

The simulations were solved using the *Continuity* software platform (UCSD NBCR, La Jolla, CA) with a double-precision solver on a Linux-based GPU cluster using a time step of 0.1 ms to solve the partial differential equation and 0.01 ms to solve ordinary differential equations of the cellular ionic model. The electrophysiology model solutions consisted of the time-varying 3D distribution of voltage in the ventricles from which the vectorcardiogram (VCG) was computed.[23] The simulated surface ECGs were derived from the VCG solutions using previously validated transformations[24, 25] and resulting simulated electrogram amplitudes for individual cycles were measured (including minor fluctuations if they represented a maximum or minimum voltage for a cycle). Cycle amplitudes were then compared using our voltage variation criteria.

Statistical Methods

Continuous variables are expressed as mean±standard deviation. Comparisons within subjects were analyzed using the paired t test; different groups were compared using the 2-sample t test. Categorical variables were compared using Fisher's Exact Test. P values <0.05 were considered significant. Statistics were calculated using R statistical software 3.3.1 (R Foundation, Vienna, Austria).

Results

We enrolled 31 subjects who were referred for ablation of ventricular tachycardia, ventricular fibrillation and/or premature ventricular contractions. VF of any duration was induced in 18 subjects. VF was sustained and required defibrillation in 14 subjects. Eight subjects, all with sustained VF, demonstrated periods of both rotors and focal sources at separate times during the VF episode and their data was used in the primary analysis. Ten subjects exhibited only one mechanism: 6 subjects demonstrated only rotors and all had sustained VF while the remaining 4 subjects demonstrated only focal sources and all had non-sustained VF. There were no significant differences in the patient characteristics of the group exhibiting both VF mechanisms compared to the group exhibiting only 1 mechanism, as shown in table 1.

Clinical Human Study

In the primary, within-subject analysis of patients exhibiting both mechanisms (n=8), rotor-based VF exhibited greater voltage variation than focal source-based VF in vector combination of orthogonal ECG leads, based on both metrics of maximal percent amplitude change (110±24% vs 55±32%, p=0.02) and standard deviation of normalized amplitudes

(0.55±0.23 vs 0.27±0.15, p=0.04) over an average electrogram duration of 2.5±1.8 seconds, as shown in table 2.

These findings were similar to our secondary analysis of all patients exhibiting any VF mechanism (n=18). Rotor-based VF exhibited greater voltage variation than focal source-based VF in vector combination of orthogonal ECG leads, based on both metrics of maximal percent amplitude change (103±30% vs 67±34%, p=0.01) and standard deviation of normalized amplitudes (0.53±0.23 vs 0.35±0.18, p=0.03) over an average electrogram duration of 3.5±2.4 seconds, as shown in table 3.

Simultaneous endocardial phase maps and orthogonal ECG leads during an episode of sustained VF driven by a focal source compared to rotors taken from a representative 52-year-old patient with ischemic cardiomyopathy are shown in Figure 2 and Video 1.

Computational Study of Rotors and Focal Sources

Controlled computational modeling (identical geometry, ionic model, model parameters, source location, and duration of VF) also found greater voltage variation in rotor-driven VF compared with focally-driven VF based on both metrics of maximal percent amplitude change (110±19% vs 33±16%, p=0.001) and standard deviation of normalized amplitudes (0.58±0.11 vs 0.15±0.08, p=0.001) over a simulated electrogram duration of 2.5 seconds, as shown in Table 4.

Complex Rotor Behavior Increases Voltage Variation

Detailed analysis of rotor behavior in the computer simulations revealed that the mechanisms of increased voltage variation could be attributed to complex rotor behavior, including wavebreak distant from the primary rotor, secondary rotor initiation, and meandering (precessing) rotors (Figure 3). To investigate this further, we simulated non-physiologic conditions by increasing conduction velocity to discourage wavebreak and found that single, stationary rotors demonstrated minimal amplitude variation compared to more physiologic VF. Specifically, analysis using metric 1 reveals that single stationary rotors without wavebreak exhibited significantly less amplitude variation (32±8%) compared to rotors with secondary rotor formation (113±26%, p=0.007) and a rotor with meander (107±14%, p=0.001). Similarly, analysis using metric 2 also reveals that single stationary rotors without wavebreak (0.08±0.02) exhibited significantly less amplitude variation compared to rotors with secondary rotor formation (0.59±0.17, p=0.007) and a rotor with meander (0.57±0.05, p=0.0001). These results are summarized in Table 5. Simulations of a focal source, non-physiologic single stationary rotor, rotor with wavebreak resulting in secondary rotor formation, and a meandering rotor are shown in Figure 3 and Video 2.

Complex Rotor Behavior Observed During Human VF

Complex behavior was frequently observed during phase mapping of human VF during rotors; wavebreak and simultaneous rotors were observed in 7 out of the 14 patients (50%) with rotors. Meander of rotors greater than 1.5 cm was observed in 11 out of 14 patients (79%). Conversely, wavebreak was largely absent during activation by focal sources. Instead, small variations in focal source location of approximately 1 interelectrode distance

(~1.5 cm) were observed. We did not observe any VF cycles in which rotors and focal sources co-existed, although we could not conclusively exclude this occurrence due to the limited resolution of basket catheter mapping.

Discussion

There are two central findings in this combined clinical and computational study. First, we quantify normalized amplitude differences between different human VF mechanisms on the surface ECG. Second, in highly controlled computer model simulations, we identify the mechanistic sources of such variations in VF ECG voltage as (a) wavebreak, (b) formation of secondary rotors at distant sites, and (c) rotor meander. These findings provide new and important insight into the mechanisms of human VF, potentially permitting non-invasive identification of the dominant mechanism in clinical VF to guide therapy.

Insights into Clinical VF

Presently, three main methods have been reported to map VF *in vivo.* The first uses an epicardial electrode array during open heart surgery,[7] The second, reported from our laboratory, uses bi-ventricular 64-electrode basket catheter inserted percutaneously during electrophysiology study to map VF and quantify rotor behavior.[10] The third uses a multielectrode vest to record body surface potentials.[11] Each has provided significant insight into the mechanisms of VF.[7, 9, 11] But each of the above techniques is costly and unlikely to be present for the vast majority of recorded clinical VF episodes. In contrast, the 12-lead ECG is routinely and continuously recorded throughout electrophysiology study involving ventricular arrhythmia induction, and in certain situations in which 12-lead telemetry is utilized.[26] However, differences in 12-lead ECG parameters between distinct VF source mechanisms had not previously been reported.

In the clinical portion of our study, we first analyzed individuals with both types of observed mechanisms: focal sources and rotors. This allowed each patient to serve as their own control to eliminate confounding factors such as cardiac anatomy, torso geometry, and subtle differences in ECG electrode positions that may have introduced bias into our analysis. We found that rotor-based VF exhibits increased voltage variability compared to focal source-based VF. We then analyzed all episodes of induced VF, and found similar results. As such, the findings from our clinical study, in patients with and without diseased myocardial substrate, are likely generalizable to patients with clinical VF. Future work should evaluate whether prospective application of these voltage criteria may identify VF mechanisms, and help plan directed therapy. Such work is currently underway in our laboratory.

Insights from Computer Modeling

Prior computational modeling work has provided key insights into the mechanisms of ventricular arrhythmias. Stevenson and colleagues used computer modeling of complex scar in the early 1990s to study entrainment mapping of ventricular tachycardia, and found that comparing the difference between post-pacing interval (PPI) and the tachycardia cycle length (TCL) can help localize the catheter to the protected isthmus or an adjacent bystander.[27] Berenfeld and colleagues used modeling to evaluate VF scroll wave filament behavior in

the presence of fiber angle anisotropy,[28] and found that filaments tend to align themselves with myocardial fibers. To date, however, computational models had not been used to examine surface ECG characteristics of different VF mechanisms.

In this work, carefully controlled simulations of human VF confirm the clinical VF ECG results. Furthermore, careful analysis of rotor behavior and simulation of non-physiologic conditions without distal wavebreak allows us to identify the precise mechanisms of voltage variation during VF. Notably, in non-physiologic simulations, the presence of an isolated, stationary rotor without distal wavebreak showed minimal surface ECG variation. This is an unexpected finding, as we had previously hypothesized that the interaction of spiral wave arms in distal tissue would still exhibit significant amplitude variation. Instead, we have determined that increased voltage variation during rotor-driven VF is due to dynamic changes in the net electrical activation from wavebreak, secondary rotor formation, and rotor meander. Importantly, such complex behavior was also observed in clinical VF, further supporting our simulation results. These findings represent novel insight into VF mechanisms.

Significance and Future Studies

Knowledge regarding the dominant mechanism underlying VF based upon widely available surface ECG recordings may be used to help guide targeted therapy for VF. For example, for VF characterized by uniform ECG amplitudes and low variability, our findings suggest that there is a dominant focal-source mechanism. Such sources can potentially be treated with medications targeting triggered activity or afterdepolarizations,[29] targeted ablation of rapid Purkinje[30, 31] and myocardial sources,[32] or ablation of intramural reentry sites that manifest as focal activation during endocardial mapping, although at present is challenging to differentiate between such mechanisms.

Conversely, a VF ECG characterized by increased voltage variability suggests rotor-driven VF, which may in the future be treated by therapies suppressing functional reentry.[33] Recent work from our lab[9] and others[11] has shown promising outcomes from ablation of dominant rotor sites. We believe that the development of new criteria to guide targeted therapy of VF has the potential to greatly improve the morbidity and quality of life for patients with clinical VF; future studies should examine whether targeted therapy directed by ECG findings improves VF outcomes.

Limitations

First, the sample size of the clinical study is limited due to challenges associated with basket mapping of VF. We further reduced the sample size in the primary analysis to patients exhibiting both VF mechanisms in order to serve as their own controls. Importantly, because similar results were identified in both the self-controls and the secondary analysis of the entire study population with induced VF, our findings are likely generalizable to patients with clinical VF. Furthermore, our clinical findings were confirmed by computational modeling studies using model parameters for VF that produced physiologic VF cycle lengths and complex behavior similar to that observed clinically using endocardial mapping. A second limitation is that a monodomain electrophysiology model was used in order to

optimize computing efficiency; such models do not factor in the contributions of cardiac extracellular space to impulse generation and propagation. Notably, prior work comparing monodomain and bidomain models on impulse propagation have shown no significant differences in computed electrograms.[34] Third, the electrophysiology model utilizes a phenomenological ionic model (Fenton-Karma) rather than a biophysical ionic model such as Ten-Tusscher in order to enable efficient computation of a large biventricular mesh. However, the present work analyzes net phenomenological mechanisms such as propagation of spiral waves and focal sources through tissue, attributable to the overall shape of the action potential waveform, which is reliably modeled by Fenton-Karma. Furthermore, implementation of an ionic model similar to ten Tusscher would be cost-prohibitive due to the intense computing requirements. Notably, the agreement in findings between observed clinical data and simulation findings is high, providing increased confidence in our results.

Conclusions

We conclude that rotor-driven VF exhibits greater surface ECG amplitude variation than focal source-driven VF. We also conclude that such differences are likely due to wavebreak, the formation of secondary rotors, and rotor meander. These findings may help classify underlying organized VF mechanisms using the widely available surface ECG. Such information may be useful for guiding optimal therapy for VF such as antiarrhythmic medications or planning VF substrate ablation procedures; prospective studies using surface ECG voltage variation criteria for VF mechanisms are required to validate these findings and to evaluate the effectiveness of interventions guided by these results. Such studies are currently underway.

Supplementary Material

Refer to Web version on PubMed Central for supplementary material.

Acknowledgments

Dr. Krummen has received grant support from the American Heart Association (10 BGIA 3500045) and NIH (HL 83359). Dr. Ho has received grant support from the UCSD Clinical Translational Research Institute: Galvanizing Engineering in Medicine Grant. Dr. Villongco has received grant support from the NIH Training Grant.

References

1. Cobb LA, Fahrenbruch CE, Olsufka M, Copass MK. Changing incidence of out-of-hospital ventricular fibrillation, 1980-2000. JAMA. 2002; 288:3008–13. [PubMed: 12479765]
2. Kong MH, Fonarow GC, Peterson ED, Curtis AB, Hernandez AF, Sanders GD, Thomas KL, Hayes DL, Al-Khatib SM. Systematic review of the incidence of sudden cardiac death in the United States. Journal of the American College of Cardiology. 2011; 57:794–801. [PubMed: 21310315]
3. Davidenko JM, Pertsov AV, Salomonsz R, Baxter W, Jalife J. Stationary and drifting spiral waves of excitation in isolated cardiac muscle. Nature. 1992; 355:349–51. [PubMed: 1731248]
4. Filgueiras-Rama D, Jalife J. Structural and Functional Bases of Cardiac Fibrillation. Differences and Similarities between Atria and Ventricles. JACC Clin Electrophysiol. 2016; 2:1–3. [PubMed: 27042693]
5. Gray RA, Jalife J, Panfilov AV, Baxter WT, Cabo C, Davidenko JM, Pertsov AM. Mechanisms of cardiac fibrillation. Science. 1995; 270:1222–3. [PubMed: 7502055]

6. Gray RA, Pertsov AM, Jalife J. Spatial and temporal organization during cardiac fibrillation. Nature. 1998; 392:75–8. [PubMed: 9510249]
7. Nash MP, Mourad A, Clayton RH, Sutton PM, Bradley CP, Hayward M, Paterson DJ, Taggart P. Evidence for multiple mechanisms in human ventricular fibrillation. Circulation. 2006; 114:536–42. [PubMed: 16880326]
8. Hayase J, Tung R, Narayan SM, Krummen DE. A case of a human ventricular fibrillation rotor localized to ablation sites for scar-mediated monomorphic ventricular tachycardia. Heart Rhythm. 2013; 10:1913–6. [PubMed: 23911894]
9. Krummen DE, Hayase J, Vampola SP, Ho G, Schricker AA, Lalani GG, Baykaner T, Coe TM, Clopton P, Rappel WJ, Omens JH, Narayan SM. Modifying Ventricular Fibrillation by Targeted Rotor Substrate Ablation: Proof-of-Concept from Experimental Studies to Clinical VF. J Cardiovasc Electrophysiol. 2015; 26:1117–26. [PubMed: 26179310]
10. Krummen DE, Hayase J, Morris DJ, Ho J, Smetak MR, Clopton P, Rappel WJ, Narayan SM. Rotor stability separates sustained ventricular fibrillation from self-terminating episodes in humans. J Am Coll Cardiol. 2014; 63:2712–21. [PubMed: 24794115]
11. Cochet H, Dubois R, Sacher F, Derval N, Sermesant M, Hocini M, Montaudon M, Haissaguerre M, Laurent F, Jais P. Cardiac arrythmias: multimodal assessment integrating body surface ECG mapping into cardiac imaging. Radiology. 2014; 271:239–47. [PubMed: 24475841]
12. Reed MJ, Clegg GR, Robertson CE. Analysing the ventricular fibrillation waveform. Resuscitation. 2003; 57:11–20. [PubMed: 12668294]
13. Cao JM, Qu Z, Kim YH, Wu TJ, Garfinkel A, Weiss JN, Karagueuzian HS, Chen PS. Spatiotemporal heterogeneity in the induction of ventricular fibrillation by rapid pacing: importance of cardiac restitution properties. Circ Res. 1999; 84:1318–31. [PubMed: 10364570]
14. Nair K, Umapathy K, Farid T, Masse S, Mueller E, Sivanandan RV, Poku K, Rao V, Nair V, Butany J, Ideker RE, Nanthakumar K. Intramural activation during early human ventricular fibrillation. Circulation Arrhythmia and electrophysiology. 2011; 4:692–703. [PubMed: 21750274]
15. Narayan SM, Krummen DE, Rappel WJ. Clinical mapping approach to diagnose electrical rotors and focal impulse sources for human atrial fibrillation. J Cardiovasc Electrophysiol. 2012; 23:447–54. [PubMed: 22537106]
16. Bray MA, Wikswo JP. Considerations in phase plane analysis for nonstationary reentrant cardiac behavior. Phys Rev E Stat Nonlin Soft Matter Phys. 2002; 65:051902. [PubMed: 12059588]
17. Narayan SM, Franz MR, Lalani G, Kim J, Sastry A. T-wave alternans, restitution of human action potential duration, and outcome. J Am Coll Cardiol. 2007; 50:2385–92. [PubMed: 18154963]
18. Narayan SM, Bayer JD, Lalani G, Trayanova NA. Action potential dynamics explain arrhythmic vulnerability in human heart failure: a clinical and modeling study implicating abnormal calcium handling. J Am Coll Cardiol. 2008; 52:1782–92. [PubMed: 19022157]
19. Gonzales MJ, Sturgeon G, Krishnamurthy A, Hake J, Jonas R, Stark P, Rappel WJ, Narayan SM, Zhang Y, Segars WP, McCulloch AD. A three-dimensional finite element model of human atrial anatomy: new methods for cubic Hermite meshes with extraordinary vertices. Med Image Anal. 2013; 17:525–37. [PubMed: 23602918]
20. Aguado-Sierra J, Krishnamurthy A, Villongco C, Chuang J, Howard E, Gonzales MJ, Omens J, Krummen DE, Narayan S, Kerckhoffs RC, McCulloch AD. Patient-specific modeling of dyssynchronous heart failure: a case study. Prog Biophys Mol Biol. 2011; 107:147–55. [PubMed: 21763714]
21. Krishnamurthy A, Villongco CT, Chuang J, Frank LR, Nigam V, Belezzuoli E, Stark P, Krummen DE, Narayan S, Omens JH, McCulloch AD, Kerckhoffs RC. Patient-Specific Models of Cardiac Biomechanics. J Comput Phys. 2013; 244:4–21. [PubMed: 23729839]
22. Fenton FH, Cherry EM, Hastings HM, Evans SJ. Multiple mechanisms of spiral wave breakup in a model of cardiac electrical activity. Chaos. 2002; 12:852–892. [PubMed: 12779613]
23. Villongco CT, Krummen DE, Stark P, Omens JH, McCulloch AD. Patient-specific modeling of ventricular activation pattern using surface ECG-derived vectorcardiogram in bundle branch block. Prog Biophys Mol Biol. 2014; 115:305–13. [PubMed: 25110279]
24. Dower GE, Yakush A, Nazzal SB, Jutzy RV, Ruiz CE. Deriving the 12-lead electrocardiogram from four (EASI) electrodes. J Electrocardiol. 1988; 21(1):S182–7. [PubMed: 3216172]

25. Kors JA, van Herpen G, Sittig AC, van Bemmel JH. Reconstruction of the Frank vectorcardiogram from standard electrocardiographic leads: diagnostic comparison of different methods. Eur Heart J. 1990; 11:1083–92. [PubMed: 2292255]
26. Haissaguerre M, Shoda M, Jais P, Nogami A, Shah DC, Kautzner J, Arentz T, Kalushe D, Lamaison D, Griffith M, Cruz F, de Paola A, Gaita F, Hocini M, Garrigue S, Macle L, Weerasooriya R, Clementy J. Mapping and ablation of idiopathic ventricular fibrillation. Circulation. 2002; 106:962–7. [PubMed: 12186801]
27. Stevenson WG, Khan H, Sager P, Saxon LA, Middlekauff HR, Natterson PD, Wiener I. Identification of reentry circuit sites during catheter mapping and radiofrequency ablation of ventricular tachycardia late after myocardial infarction. Circulation. 1993; 88:1647–70. [PubMed: 8403311]
28. Berenfeld O, Wellner M, Jalife J, Pertsov AM. Shaping of a scroll wave filament by cardiac fibers. Phys Rev E Stat Nonlin Soft Matter Phys. 2001; 63:061901. [PubMed: 11415139]
29. Milberg P, Frommeyer G, Kleideiter A, Fischer A, Osada N, Breithardt G, Fehr M, Eckardt L. Antiarrhythmic effects of free polyunsaturated fatty acids in an experimental model of LQT2 and LQT3 due to suppression of early afterdepolarizations and reduction of spatial and temporal dispersion of repolarization. Heart Rhythm. 2011; 8:1492–500. [PubMed: 21459164]
30. Haissaguerre M, Shah DC, Jais P, Shoda M, Kautzner J, Arentz T, Kalushe D, Kadish A, Griffith M, Gaita F, Yamane T, Garrigue S, Hocini M, Clementy J. Role of Purkinje conducting system in triggering of idiopathic ventricular fibrillation. Lancet. 2002; 359:677–8. [PubMed: 11879868]
31. Knecht S, Sacher F, Wright M, Hocini M, Nogami A, Arentz T, Petit B, Franck R, De Chillou C, Lamaison D, Farre J, Lavergne T, Verbeet T, Nault I, Matsuo S, Leroux L, Weerasooriya R, Cauchemez B, Lellouche N, Derval N, Narayan SM, Jais P, Clementy J, Haissaguerre M. Long-term follow-up of idiopathic ventricular fibrillation ablation: a multicenter study. J Am Coll Cardiol. 2009; 54:522–8. [PubMed: 19643313]
32. Van Herendael H, Zado ES, Haqqani H, Tschabrunn CM, Callans DJ, Frankel DS, Lin D, Garcia F, Hutchinson MD, Riley M, Bala R, Dixit S, Yadava M, Marchlinski FE. Catheter ablation of ventricular fibrillation: importance of left ventricular outflow tract and papillary muscle triggers. Heart rhythm : the official journal of the Heart Rhythm Society. 2014; 11:566–73.
33. Bingen BO, Engels MC, Schalij MJ, Jangsangthong W, Neshati Z, Feola I, Ypey DL, Askar SF, Panfilov AV, Pijnappels DA, de Vries AA. Light-induced termination of spiral wave arrhythmias by optogenetic engineering of atrial cardiomyocytes. Cardiovasc Res. 2014; 104:194–205. [PubMed: 25082848]
34. Potse M, Dube B, Richer J, Vinet A, Gulrajani RM. A comparison of monodomain and bidomain reaction-diffusion models for action potential propagation in the human heart. IEEE Trans Biomed Eng. 2006; 53:2425–35. [PubMed: 17153199]

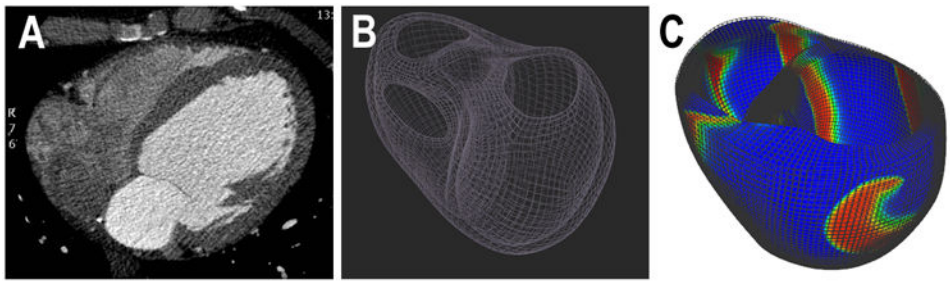

Figure 1. Realistic biventricular computer simulations were constructed from clinical computed tomographic (CT) imaging

(a) using high order cubic-Hermite finite element meshes consisting of 76,000 elements (b) from patients in the clinical study. VF is simulated with a rotor originating in the LV lateral wall as shown in (c).

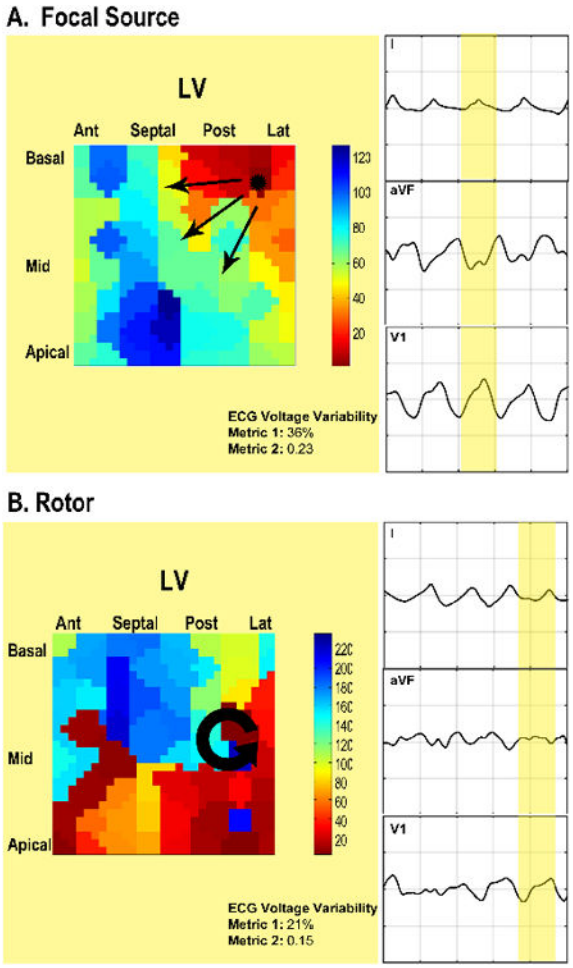

Figure 2. Comparisons of the Surface ECG during Rotor-based versus Focal source-based Human VF

ECG leads I, aVF, and V1 are shown during an episode of sustained VF induced by triple extrastimulus pacing in a 54-year-old patient with ischemic cardiomyopathy. Endocardial phase-analysis identified (a) focal activation originating from the posterolateral LV and (b) a counter-clockwise rotor originating from the posterolateral LV (a simultaneous counterclockwise rotor in the RV is not shown). Greater voltage amplitude variation is noted on the rotor-based ECG in all leads compared to the focal source-based ECG.

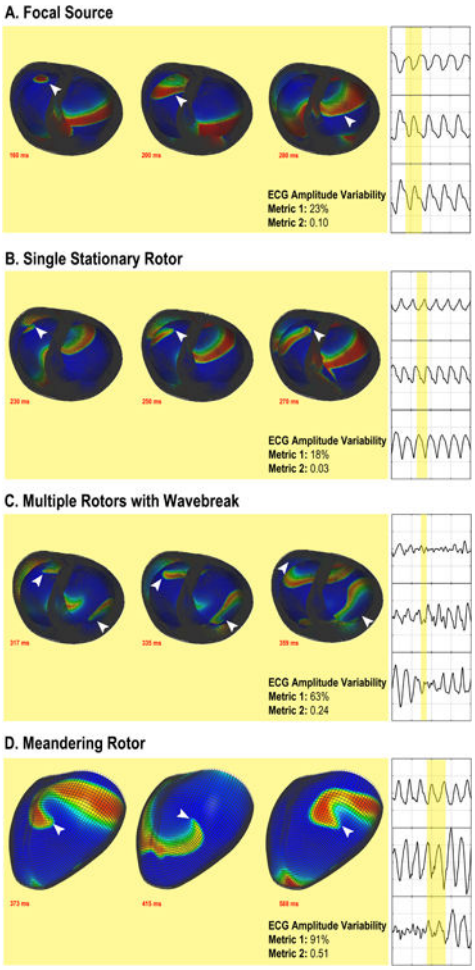

Figure 3. Comparison of ECG AmplitudeVariation BetweenComputer Simulations of Focal Sources and Rotors

Detailed biventricular computer models simulating focal sources and rotors were created. Minimal ECG amplitude variation is observed during VF with (a) focal sources and (b) single stationary rotors, while greater ECG amplitude variation occurred with (c) wavebreak with secondary rotor formation and (d) a meandering rotor. The white arrow denotes the spiral wave tip in rotor-driven VFor activation wavefrontduring focal source-driven VF.

Table 1
Baseline Clinical Characteristics of Subjects with Induced VF

Characteristics	Study population: Subjects with Both VF Mechanisms, n (%)	Subjects with a Single VF Mechanism, n (%)	P value
	N = 8	N = 10	
Age (years)	69±7	65±7	0.24
LVEF (%)	39±19	40±14	0.86
Ischemic Cardiomyopathy	4 (50%)	1 (17%)	0.30
Non-ischemic cardiomyopathy	2 (25%)	6 (60%)	0.19
Prior history of sustained VT	5 (63%)	4 (67%)	0.64
Prior history of VF	2 (25%)	0 (0%)	0.18
Indication for Procedure:			
VT/VF ablation	5 (63%)	4 (40%)	0.64
PVC ablation	3 (38%)	6 (60%)	0.64
Coronary disease	6 (75%)	5 (50%)	0.37
Prior myocardial infarction	5 (63%)	2 (20%)	0.15
Prior PCI	3 (38%)	5 (50%)	0.66
CABG	4 (50%)	2 (20%)	0.32
Hypertension	6 (75%)	9 (90%)	0.56
Diabetes mellitus	3 (38%)	1 (10%)	0.28
Hyperlipidemia	7 (88%)	8 (80%)	1
Antiarrhythmic medication	4 (50%)	2 (20%)	0.12

Table 2

Rotors Exhibit Greater ECG Voltage Variation Compared to Focal Sources For Patients Exhibiting Both Mechanisms: Primary Analysis

Maximal Percent Amplitude Difference				
	Lead 1	**Lead aVF**	**Lead V1**	**Vector Combination**
Rotor-based VF	51%±20%	63%±21%	70%±22%	**110%±24%**
Focal Source-based VF	32%±20%	25%±17%	31%±27%	**55%±32%**
p value	0.12	0.003	0.06	**0.02**
Standard Deviation of Normalized Amplitudes				
	Lead 1	**Lead aVF**	**Lead V1**	**Vector Combination**
Rotor-based VF	0.25±0.20	0.28±0.15	0.35±0.19	**0.55±0.23**
Focal Source-based VF	0.15±0.09	0.12±0.09	0.15±0.14	**0.27±0.15**
p value	0.25	0.004	0.11	**0.04**

Table 3

Rotors Exhibit Greater ECG Voltage Variation Compared to Focal Sources in All Patients: Secondary Analysis

Maximal Percent Amplitude Difference				
	Lead 1	**Lead aVF**	**Lead V1**	**Vector Combination**
Rotor-based VF	50%±25%	54%±22%	68%±20%	**103%±30%**
Focal Source-based VF	42%±21%	31%±22%	37%±27%	**67%±34%**
p value	0.34	0.02	0.002	**0.01**
Standard Deviation of Normalized Amplitudes				
	Lead 1	**Lead aVF**	**Lead V1**	**Vector Combination**
Rotor-based VF	0.25±0.18	0.27±0.15	0.35±0.16	**0.53±0.23**
Focal Source-based VF	0.21±0.12	0.17±0.14	0.18±0.13	**0.35±0.18**
p value	0.48	0.10	0.01	**0.03**

Table 4

Voltage Variation in Computer Simulations of Rotors and Focal Sources Reflects Differences Observed Clinically

Maximal Percent Amplitude Difference				
	Lead 1	**Lead aVF**	**Lead V1**	**Vector Combination**
Rotor-based VF	55±19%	56±18%	74±12%	**110±19%**
Focal Source-based VF	6±6%	21±10%	23±16%	**33±16%**
p value	0.003	0.02	0.001	**0.001**
Standard Deviation of Normalized Amplitudes				
	Lead 1	**Lead aVF**	**Lead V1**	**Vector Combination**
Rotor-based VF	0.27±0.1	0.27±0.11	0.42±0.1	**0.58±0.11**
Focal Source-based VF	0.02±0.03	0.09±0.05	0.11±0.08	**0.15±0.08**
p value	0.005	0.033	0.002	**0.001**

Table 5

Secondary Rotor Formation and Rotor Meander Increases ECG Voltage Variability

Maximal Percent Amplitude Difference		
	Vector Combination	**P value**
Single Stationary Rotor	32±8%	
Secondary Rotor Formation	113±26%	0.007
Meandering Rotor	107±14%	0.001
Standard Deviation of Normalized Amplitudes		
	Vector Combination	**P value**
Single Stationary Rotor	0.08±0.02	
Secondary Rotor Formation	0.59±0.17	0.007
Meandering Rotor	0.57±0.05	0.0001